

# Technologies for Pollution Control

## Membrane Processes

**KEYWORDS:** Pressure-Driven Membrane Process / Liquid-Liquid Membrane Contactor / Nano-Enhanced Membranes

**New membrane-based systems for seawater desalination and tertiary treatment of urban wastewaters, targeting the removal of contaminants of emerging concern.**

### Objectives

The main goal of this activity is related to the design and evaluation of two membrane reactors using functionalized membranes for water purification. The membrane reactors are distinguished by their modes of operation: (i) pressure-driven membrane process (PMP; the membrane acts as a filter medium and catalyst support), and (ii) liquid-liquid membrane contactor (LLMC; the membrane acts as oxidant injector and catalyst support).

### Current Development

Photocatalytic membrane reactors (PMRs) were applied for tertiary treatment of urban wastewater towards the removal of contaminants of emerging concern (CECs) under the NOR-WATER project ([www.nor-water.eu](http://www.nor-water.eu)). Nano-engineered membranes (NEM) were prepared and assembled in two innovative PMRs.

Configuration A consists of a ceramic tubular NEM internally fed with liquid oxidants (hydrogen peroxide ( $\text{H}_2\text{O}_2$ ) or persulfate ( $\text{S}_2\text{O}_8^{2-}$ )) and with the catalyst (titanium dioxide ( $\text{TiO}_2$ ) or silver molybdate ( $\text{Ag}_2\text{MoO}_4$ )) embedded onto the membrane shell-side (Fig 1). Polluted water is continuously fed into the annular space between the NEM shell-side and an outer quartz tube. Radiation is externally supplied via four ultraviolet C (UVC) lamps spaced equidistantly around the reactor. The oxidant permeates through the membrane pores, being efficiently dosed and uniformly delivered to the active catalyst sites, reducing its consumption, improving contact with the pollutants, and avoiding catalyst deactivation. The inlet and outlet of the water stream are located tangentially to the inner wall of the external tube, inducing a helical movement of water around the membrane shell-side. This movement increases the oxidant radial dispersion, resulting in a more homogeneous distribution of the oxidant in the annular reaction zone (ARZ), enhancing its UVC photolytic cleavage into powerful reactive species. The same approach was used to promote a highly efficient photo-Fenton (PF) process at neutral pH under continuous mode operation. In this case, a concentrated acidic  $\text{Fe}^{2+}$  solution is internally fed to a ceramic ultrafiltration membrane, permeating through the membrane pores (inside-out mode), being dosed and uniformly delivered to the membrane shell-side. Polluted water, containing CECs and oxidant ( $\text{H}_2\text{O}_2$  or  $\text{S}_2\text{O}_8^{2-}$ ), is continuously fed into the annular space between the inner membrane tubing and outer quartz tubing. The virtually unlimited number of  $\text{Fe}^{2+}$  dosing points across the membrane length, where small doses of  $\text{Fe}^{2+}$  are delivered to the reaction medium, allows for a more homogeneous distribution of the catalyst solution in the ARZ and better contact between UV photons and photoactive ferric iron species, promoting partial regeneration back to ferrous iron, and resulting in uniform pollutants conversion rates over the reactor length. Additionally, the acidic ferrous iron solution, internally fed to the membrane, allows for local points near the membrane shell-side with acidic pH values, allowing a more efficient regeneration of ferric to ferrous ions with the UV light,

minimizing the precipitation of iron near the membrane and enhancing the production of reactive oxygen species.

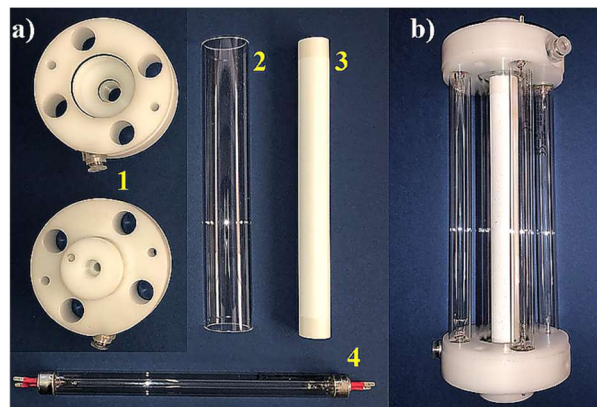


Fig 1. Photographs of the tube-in-tube reactor b) and respective components a): 1 - polypropylene flanges; 2 - quartz outer tube; 3 -  $\gamma$ - $\text{Al}_2\text{O}_3$  ultrafiltration membrane inner tube; 4 - UVC lamp.

Configuration B consists of a ceramic tubular NEM for concurrent oxidation and separation of pollutants (Fig 2). In this reactor, the NEM plays both the role of CECs barrier (pressure filtration) and oxidation, presenting several advantages, such as: (i) enhanced membrane permeability and hydrophobicity; (ii) reduced catalyst loss; and (iii) improved antifouling membrane properties through CECs and natural organic matter oxidation, leading to a high-quality permeate, which can be used for irrigation purposes, and a concentrate (membrane rejection) with a lower organic load.

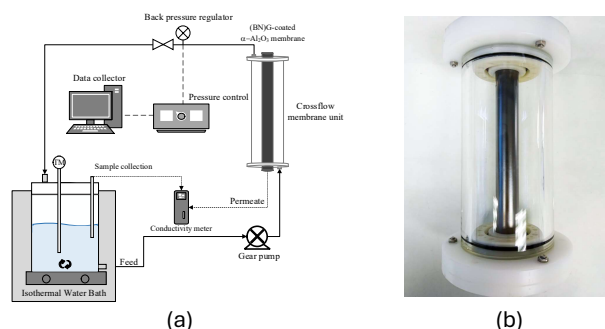


Fig 2. Schematic diagram of the laboratory-scale cross-flow membrane filtration unit (a) and photograph of the membrane module (b).

Using configuration A, a tubular ceramic ultrafiltration membrane coated with  $\text{TiO}_2$ -P25 or  $\text{Ag}_2\text{MoO}_4$  was applied in the studies with the dosage of liquid oxidants ( $\text{H}_2\text{O}_2$  or  $\text{S}_2\text{O}_8^{2-}$ ). This novel tube-in-tube membrane photoreactor, operated in continuous mode, was used to remove 19 CECs (with an initial concentration of  $10 \mu\text{g L}^{-1}$  for each) spiked in urban wastewater (UWW) after secondary treatment. The CECs were selected under the NOR-WATER project based on their occurrence in the water cycle (North of Portugal and Galicia), persistence during treatment, bioaccumulation, and toxicity to health and environment. For the photocatalytic processes using liquid oxidants, the  $\text{Ag}_2\text{MoO}_4/\text{UVC}/\text{S}_2\text{O}_8^{2-}$  system showed the best results, with more than 80% removal for 12 of the 19 CECs in UWW, considering a recirculation ratio of 11 (residence time of 73 s). Similar work was performed in collaboration with the CRETUS Institute (Department of Analytical Chemistry, Nutrition and Food Science, University

of Santiago de Compostela, Spain), using a mixture of 14 antibiotics (50  $\mu\text{g L}^{-1}$  of each). The  $\text{Ag}_2\text{MoO}_4/\text{UVC}/\text{S}_2\text{O}_8^{2-}$  system operated in a continuous flow with a residence time of 6 s, oxidant concentration of 1.2 mM, and photonic flux of  $1.7 J_{\text{UVC}} \text{ s}^{-1}$ , enabled the removal of 5 antibiotics above 60%.

The tubular membrane photoreactor, operated in continuous mode, was also used to promote the PF ( $\text{UVC}/\text{Fe}^{2+}/\text{H}_2\text{O}_2$ ) and PF-like ( $\text{UVC}/\text{Fe}^{2+}/\text{S}_2\text{O}_8^{2-}$ ) processes under near-neutral pH conditions for the oxidation of 19 CECs in the tertiary treatment of UWW. Although certain short-chain PFAS and the artificial sweetener saccharine exhibited their recalcitrant character to all conditions tested, the PF-like process demonstrated superior oxidation capacity when compared with the PF process, achieving higher removals for most target contaminants, particularly for melamine (retention time = 73.2 s,  $[\text{Fe}^{2+}] = 5 \text{ mg L}^{-1}$ , and  $[\text{oxidant}] = 1.2 \text{ mM}$ , PF process removed 7 CECs >60% and PF-like 10 CECs >60%). The activation of  $\text{S}_2\text{O}_8^{2-}$  not only induces pH decay, contributing to the permanence of dissolved iron species as verified by the lower precipitation of phosphate, but is also able to generate both  $\text{SO}_4^{\cdot-}$  and  $\text{HO}^{\cdot}$  radicals that can act in complementary oxidation pathways boosting CECs degradation. Moreover, the continuous "titration" of small catalyst doses permits a low final iron concentration, which is important for meeting discharge limits or water reuse purposes. In addition to removing micropollutants, the simultaneous removal of  $\text{PO}_4^{3-}$  through the formation of strengite appears to be a further advantage, being fundamental in introducing reuse, recycling, and resource recovery paradigms in wastewater management.

Regarding configuration B, continuous Graphene (G)- $\text{TiO}_2$  nanocomposite thin-films over a ceramic microfiltration membrane were obtained through a facile and single-step method using chitosan as a precursor to graphene production.

Microfiltration ceramic membranes were coated in situ with graphene (G)- $\text{TiO}_2$ -P25 nanocomposite using two different methods: Membrane type A -  $\text{TiO}_2$ -P25 incorporated in the G preparation stage (1% [MA-1], 2% [MA-2] and 3% [MA-3] [w/v]), and Membrane type B -  $\text{TiO}_2$ -P25 thin-film uniformly coated over the G film surface (coating layers: 3 [MB-1], 6 [MB-2], and 9 [MB-3]). After catalyst deposition and before the pyrolysis step, the air was forced to pass through the membrane's pores (inside-outside mode), providing a porous film. The membrane type A resulted in a continuous film of G interspersed with aggregates of  $\text{TiO}_2$ , creating a discontinuity in the G layer, which allows more defects in the catalyst film. Membrane type B results in a continuous G layer covered by  $\text{TiO}_2$  nanoparticles. MA-3 (type A) presents a hydraulic permeability nearly three times higher than MB-2 (type B), mainly associated with its higher porosity, mean pore size, and intrinsic hydrophilicity character. The PMR with the functionalized membranes, activated by UVA light, operated in a single-pass flow-through mode for the treatment of synthetic CECs solutions, exhibits a substantial improvement in the membrane permeate quality and quantity compared to its performance in the absence of light. The G- $\text{TiO}_2$ -UVA systems present high stability for at least 12 hours of continuous operation and reduced reversible and irreversible fouling due to the synergetic functions of CECs' oxidation and self-cleaning process. Overall, the results in this study indicate that the G- $\text{TiO}_2$ -UVA systems investigated achieved good removal of CECs and were able to reduce

CECs toxicity to zebrafish embryos effectively. Membrane type B enables a slightly higher CECs rejection than membrane type A, which can be explained mainly by its better exposure of the photocatalyst to light. However, the accumulation of the nanoparticles over the G film increases the surface roughness of membrane MB-2, confirmed by AFM analysis, reducing its resistance to fouling when compared to membrane MA-3. CECs rejection followed the sequence  $\text{E2} > \text{EE2} > \text{DCF} > \text{AMX}$ . In the absence of light, the rejection is mainly associated with size exclusion for E2 and EE2 (neutral molecules; fairly hydrophobic) and the Donnan exclusion effect for the negatively charged DCF and AMX molecules. In the presence of light, the rejection of CECs can be correlated with their reactivity towards hydroxyl radicals and higher driving force for the catalyst surface. Although the UWW matrix showed a significant negative effect on permeate flux when compared to the synthetic solution prepared with ultrapure water (UPW), mainly due to the presence of substances that may deposit or adsorb onto the membrane's surface (blocking the membrane pores), the decline in the CECs rejection was not significant when compared with the synthetic CECs solution.

A new concept for preparing large-area membranes, based on the on-site formation of multilayer defective graphene (G), was investigated for water desalination using the PMP. The desalination membrane was prepared using a continuous film of multilayer boron nitride (BN)-codoped defective G on a porous (100 nm)  $\alpha\text{-Al}_2\text{O}_3$  membrane as support. The thermal stability of the ceramic  $\alpha\text{-Al}_2\text{O}_3$  makes possible the preparation of defective multilayer (B,N)G by pyrolysis of chitosan (CS) containing adsorbed  $(\text{NH}_4)_3\text{BO}_3$ . The partial removal of B and N dopant atoms by  $\text{H}_2$  during the pyrolysis causes the generation of subnanometric pores due to atom vacancy, as determined by control experiments in the absence of this gas. NaCl and KCl removal efficiency from brackish water greater than 95% was obtained for a permeate flux of  $24.3 \text{ L m}^{-2} \text{ h}^{-1}$  at 10 bar. Due to the excellent rejection rate of NaCl and KCl from brackish water and high permeate flux at lower transmembrane pressure, as well as the large area, the membrane reported herein appears to be easy to implement in water desalination and other membrane filtration applications.

#### Future Perspectives

NEWater project, supported by the Water4All program: Integration of ozonation, biofiltration, and membrane filtration (ultrafiltration and reverse osmosis) for the treatment of secondary municipal wastewater, enabling the production of a high-quality permeate for electrolysis.

#### Related Sustainable Development Goals



#### Outputs

##### PhD Theses

- [1] Jonathan Cawettiere Almeida Espíndola, Innovative photochemical/photocatalytic reactors towards micropollutants mitigation, PDEA, FEUP, 2019
- [2] Reynel Martínez Castellanos, Simultaneous removal of nutrients and endocrine disrupting chemicals by aerobic granular sludge and advanced oxidation processes, PDEA, FEUP/UFRJ, 2020
- [3] Lúcio Melchades Gomes, Advanced technologies for the removal of contaminants of emerging concern from urban wastewaters, PDEA, FEUP, on-going, 2020-2024

### **Master Dissertations**

[1] Carla de Sousa Santos, Foto-Fenton a pH neutro usando um foto-reator de membrana tubular para dosagem radial de Fe(II): Avaliação da degradação de contaminantes de preocupação emergente em águas residuais, MIEA, FEUP, 2022

### **Selected Publications**

[1] P.H. Presumido et al., Chem. Eng. J. 430, 132639 (2022)

[2] L. Vazquez et al., J. Environ. Chem. Eng. 11, 109766 (2023)

[3] C. Santos et al., Chem. Eng. J. 476, 146655 (2023)

### **Team**

**Vitor Vilar** Principal Researcher; Ana Isabel Gomes Junior Researcher; **Jonathan Espíndola**, PhD Student; **Lúcio Gomes**, PhD Student; **Reynel Castellanos**, PhD Student; **Carla Santos**, Master Student

### **Funding**

NOR-WATER, 0725\_NOR\_WATER\_1\_P, 2019-2022

LSRE-LCM Base Funding, UIDB/50020/2020, 2020-2023

LSRE-LCM Programmatic Funding, UIDP/50020/2020, 2020-2023

LA LSRE-LCM Funding, UID/EQU/50020/2019, 2019

LA LSRE-LCM Funding, POCI-01-0145-FEDER-006984, 2013-2018

FCT Grants: CEECIND/01317/2017

FCT Scholarships: CNPq/205781/2014-4, CNPq: 870073/1997-4